OPEN ACCESS
IOP Publishing
Measurement Science and Technology
Meas. Sci. Technol. **33** (2022) 094006 (9pp)
https://doi.org/10.1088/1361-6501/ac74a1

Electrical resistance tomography-based multi-modality sensor and drift flux model for measurement of oil–gas–water flow

Sara Rashed[1], **Yousef Faraj**[1,*], **Mi Wang**[2] **and Stephen Wilkinson**[1]

[1] Department of Chemical Engineering, University of Chester, Chester, United Kingdom
[2] School of Chemical and Process Engineering, University of Leeds, Leeds, United Kingdom

E-mail: y.faraj@chester.ac.uk

Received 8 January 2022, revised 14 May 2022
Accepted for publication 30 May 2022
Published 14 June 2022

Abstract

This paper proposes a novel method to measure each constituent of an oil–gas–water mixture in a water continuous flow, typically encountered in many processes. It deploys a dual-plane electrical resistance tomography sensor for measuring dispersed phase volume fraction and velocity; a gradiomanometer flow density meter and a drift flux model to estimate slip velocities; with absolute pressure and temperature measurements. These data are fused to estimate constituent volume flow rates. Other commonly used operational parameters can be further derived: water cut or water liquid ratio (WLR) and gas volume fraction (GVF). Trials are described for flow rates of water 5–10 $m^3\ h^{-1}$; oil 2–10 $m^3\ h^{-1}$ and gas 1–15 $m^3\ h^{-1}$. The comparative results are included with published data from the Schlumberger Gould Research flow facility. The paper proposes the use of the described configuration for measurement of volume flow rates in oil–gas–water flows with an absolute error of $\pm 10\%$ within GVF 9%–85% and WLR > 45%.

Keywords: three-phase flow measurement, vertical upward flow, oil–gas–water flow, flow metering, electrical resistance tomography, drift flux model

(Some figures may appear in colour only in the online journal)

1. Introduction

Three-phase streams of oil, gas and water are commonly encountered in the transportation pipelines, flow lines associated with oil production, dehydration units and much other processing equipment [1–3]. Various multi-modality sensors and methods have been reported for multiphase flow measurement such as dual-modality electrical resistance tomography (ERT) and electromagnetic flowmeter (EMF) [1], Venturi meter with blind tee and gamma ray system [4], x-ray tube and group method of data handling [5] and so on. While multiphase measurement techniques have increased in number, the problem of how to measure the oil–gas–water mixture in pipelines in an accurate, fast, cost-effective and safe manner remains among the key challenges. In parallel with the development of more complex production techniques, flow metering requirements correspondingly are increasing, resulting in increased range, rapid measurement, reduced measurement uncertainty,

* Author to whom any correspondence should be addressed.

reduced capital and operational cost, and enhanced long-term reliability.

The complex nature of multiphase flow emphasises the importance of accurate flow parameter measurements such as velocities, volume fractions, pressure, temperature, and operational parameters, including gas volume fraction (GVF). Accurate estimation of these parameters is essential for determining the phase volume flow rates. In practice, the traditional separation method and gamma-ray techniques are used to determine the flow rate of individual phases within three-phase mixture [6]. The separation method is widely used in the oil production industry; however, it is an expensive, time-consuming, and bulky process within the industry. Although gamma-ray is reported to be an elegant and highly accurate measurement technique, it is an unsafe and costly technique [6].

Novel methods have recently been proposed for measuring oil–gas–water flows, such as electrical impedance tomography (EIT) in combination with EMF and flow density metering (FDM) in vertical upward flow [7]; combined electrical and ultrasonic sensors in horizontal water-based flow [3] and so on. Such methods measure three-phase flow rate in a safe manner; however, they utilise multiple expensive instruments, resulting in an increased capital and maintenance costs. Furthermore, the EIT-EMF-FDM measurement technique does not account for the phase slippage effect, while the combined electrical and ultrasonic sensor method is limited to the wavy flow pattern.

The ERT is an imaging technique that images the distribution of conductivity in a pipe or vessel cross-sectional area, which can be converted to local volume fraction of the dispersed phase using the Maxwell relationship [1]. The ERT technique is considered a good choice for multiphase flow measurement, as it is non-invasive, safe (i.e. radioactive-free) and provides accurate and rapid measurements. ERT has previously been used for multiphase flow measurement as a non-invasive and rapid tool to interrogate the internal structure of multiphase flow. Faraj *et al* developed a dual-multi-modality ERT and EMF sensor to measure phase flow rates in two-phase oil–water mixtures with an absolute error of $\pm 2\%$ [1]. Qureshi *et al* used ERT for examining horizontal three-phase flow, air, liquid and solid at a wide range of operating conditions [8]. It has also been used successfully for the measurement of phase holdup, phase distribution and phase propagation velocity of three-phase gas, liquid and solid [9].

The drift flux model (DFM) is a practical and precise two-phase flow model that can be used to analyse either gas–liquid or oil–water. This model, which has been widely applied to multiphase flows [10], considers the relative motion between phases using a fundamental relation. It has been used in engineering applications and for studying two- and three-phase flow by Abam *et al* [11], Soprana *et al* [12], and Dong *et al* [13].

Despite the increased number of multiphase flow measurement techniques reported in the literature, further studies in developing a cost-effective, rapid, accurate, and non-invasive method to determine phase volume flow rate within oil–gas–water flow is necessary, particularly in which the phase slip velocity is addressed. This paper aims to propose a novel multiphase flow measurement method, in which ERT is combined with FDM and DFM to measure each constituent volume flow rate within the multiphase mixture non-invasively considering the slip velocities.

2. Measurement concept and methodology

The novel oil–gas–water flow measurement concept that is developed in this work is illustrated in figure 1. In the oil–gas–water flow system, the dual-plane ERT sensor is used as a non-invasive tool for interrogating the internal structure of the pipe flow, producing the dispersed phase volume fraction and velocity. The ERT velocity measurements are obtained using pixel to pixel cross-correlation of reconstructed images [7]. Since ERT measures the combined mean volume fraction, $\overline{\boldsymbol{\alpha}}_{\boldsymbol{d}}$, and velocity $\boldsymbol{v_d}$ of the dispersed phase (i.e. oil and gas), it is combined with FDM and DFM to determine the volume fraction and velocity of each constituent phase, considering slip velocity, using the following equations (1)–(6):

$$\bar{\alpha}_o = \left(\frac{\rho_C}{\rho_O - \rho_G}\right)\left[\frac{\Delta P}{\rho_C h_p\left[g\cos\theta + \frac{2C_f V_m^2}{D}\right]} + \bar{\alpha}_d\left(\frac{\rho_C + \rho_G}{\rho_C}\right) - 1\right] \tag{1}$$

$$\bar{\alpha}_d + \bar{\alpha}_w = 1 \tag{2}$$

$$\bar{\alpha}_g = \bar{\alpha}_d - \bar{\alpha}_o \tag{3}$$

$$v_g = \frac{V_g' d - C_o V_r \bar{\alpha}_d - \bar{\alpha}_d v_d}{1 - C_o \bar{\alpha}_c} \tag{4}$$

$$v_o = v_g\left(1 - C_o \bar{\alpha}_g\right) + V_o' d \tag{5}$$

$$v_w = V_{sl} - \bar{\alpha}_{ol} v_r' / \left(\bar{\alpha}_{ol} + \bar{\alpha}_{wl}\right) \tag{6}$$

where $\bar{\alpha}_o$, $\bar{\alpha}_g$, $\bar{\alpha}_w$, v_o, v_g, v_w, are the oil, gas and water volume fractions and velocities, respectively. ρ_C, ρ_O, ρ_G are the densities of the water, oil and gas phases, respectively. Since the gas density varies with temperature and pressure due to compressibility, $\rho_G = \rho_{Gs}\left(\frac{P_A}{T_A}\right)\left(\frac{T_S}{P_S}\right)$ is used to correct the gas density (assuming it is an ideal gas) based on the actual temperature (T_A) and actual pressure (P_A), where ρ_{Gs}, T_S and P_S are the density, temperature and pressure of the gas at standard conditions. ΔP is the pressure drop C_f is the friction factor. h_p , D and θ are the pipe height, diameter, and the inclination angle (which is 0 in vertical flow), respectively. V_m, V_{sl}, v_r, v_r' and $V_g' d$ are the mixture velocity, liquid mixture velocity, gas–liquid and water–oil relative velocities and gas drift velocity, respectively. $\bar{\alpha}_{ol}$ and $\bar{\alpha}_{wl}$ are the mean oil and water volume fractions in the liquid phase.

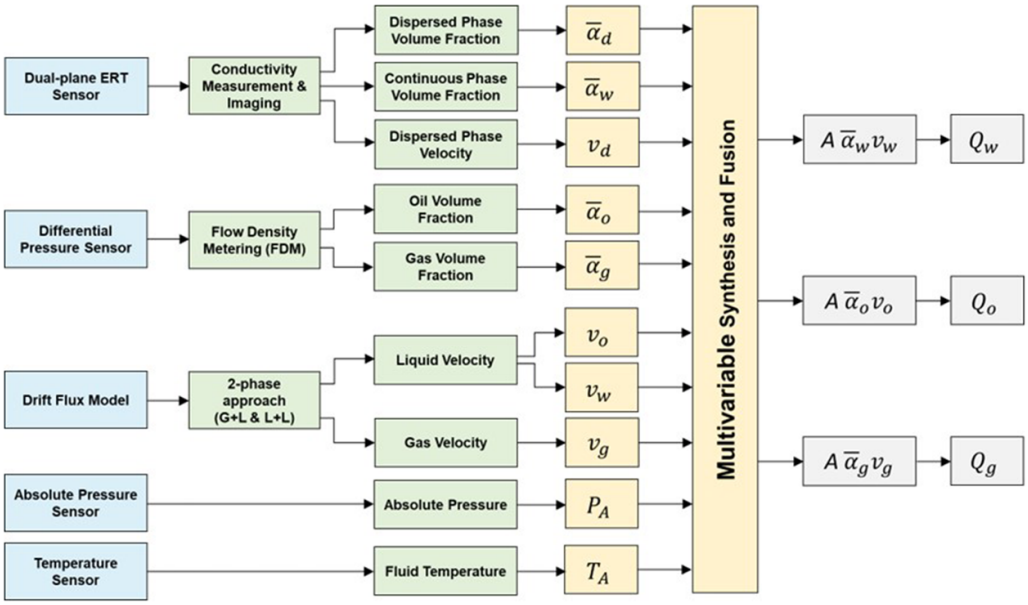

Figure 1. Schematic diagram of measurement concept.

Each phase volume flow rate is then determined as the product of phase volume fraction, phase velocity and pipe cross-sectional area, A, as shown in equations (7)–(9):

$$Q_g = A\bar{\alpha}_g v_g \tag{7}$$

$$Q_o = A\bar{\alpha}_o v_o \tag{8}$$

$$Q_w = A\bar{\alpha}_w v_w. \tag{9}$$

The performance of the measurement technique proposed in this paper is evaluated based on the experimental reference values published in Wang *et al* [7], in which a series of experiments were carried out using the Schlumberger Gould Research (SGR) inclinable flow facility. As part of this study's evaluation of our proposed measurement strategy, the inlet phase flow rates that were introduced to the flow facility are used as a reference. Wang *et al* reported that they utilised low-viscosity oil fluid (Total-D75 Kerosene, 2 cP), nitrogen gas and tap water at a wide range of conditions in vertical upward flow while testing their ERT-FDM-DFM multi-modality sensor system. The range of kerosine, nitrogen and water inlet flow rates were 5–10 $m^3\ h^{-1}$, 2–10 $m^3\ h^{-1}$ and 1–15 $m^3\ h^{-1}$, respectively. The tests were carried out within the temperature range of 15 °C–20 °C using a pipe diameter (D) and height (h_p) of 0.05 m and 0.65 m, respectively, were utilised. Table 1 shows the parameters used in evaluating the proposed method, in which the viscosity values are those at 20 °C and 1bar, and the local tap water reference conductivity is at 20 °C.

Table 1. Summary of the parameters used in oil–gas–water measurements.

Oil flow rate range ($m^3\ h^{-1}$)	5–10
Water flow rate range ($m^3\ h^{-1}$)	1–15
Gas flow rate range ($m^3\ h^{-1}$)	2–10
Pipe diameter (m)	0.05
Pipe height (m)	0.65
Oil viscosity (pa·s)	0.002
Water viscosity (pa·s)	0.001
Gas viscosity (pa·s)	1.76×10^{-5}
Average actual pressure (bar)	2
Average actual temperature (°C)	18.7
Standard pressure (bar)	1
Standard temperature (°C)	20
Gravitational acceleration, g ($m\ s^{-2}$)	9.81
Surface tension σ_{o-w} ($N\ m^{-1}$)	0.0335
Gas density ($kg\ m^{-3}$)	1.165
Water density ($kg\ m^{-3}$)	1000
Water reference conductivity ($mS\ cm^{-1}$)	0.7
Oil density ($kg\ m^{-3}$)	810

2.1. Proposed dual-plane ERT-based multi-modality sensor

This work proposes a dual-plane ERT-based multi-modality sensor configuration, as illustrated in figure 2. The proposed system is a product of integrating several subsystems into a robotic, rigid flow meter for metering three-phase flow. The integrated system is approximately 1 m long with 50 mm internal diameter and consists of a dual-plane ERT sensor, an off-the-shelf differential pressure sensor, two absolute pressure sensors and a temperature sesnor. Each ERT plane sensor

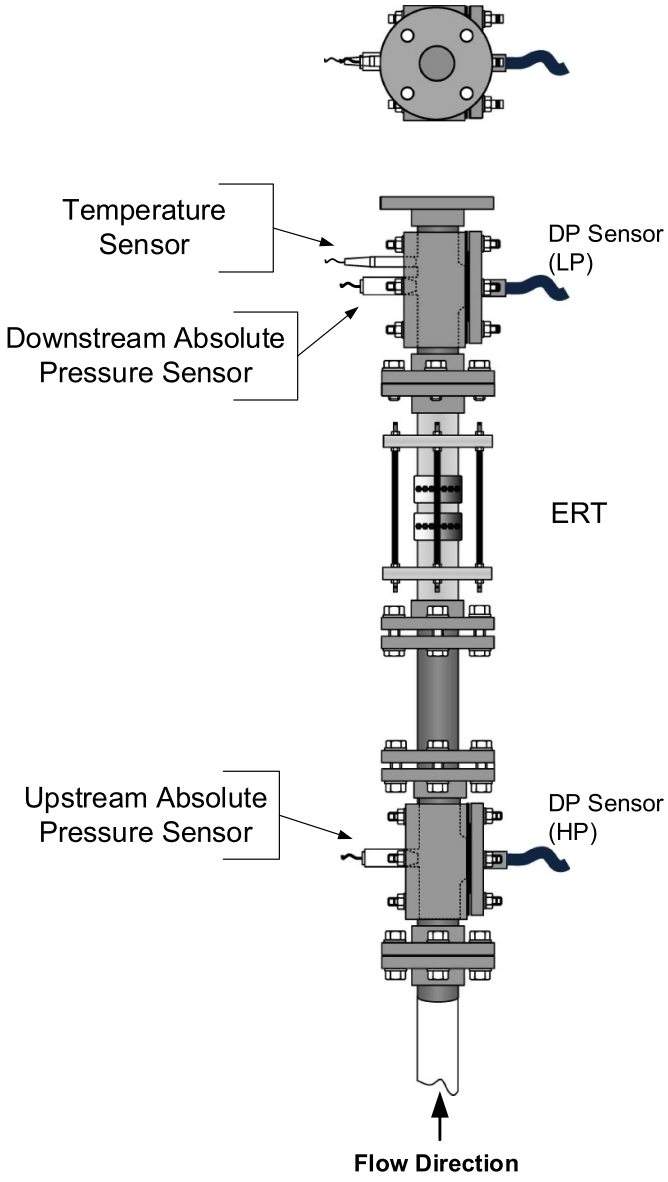

Figure 2. Proposed dual-plane ERT-based multi-modality sensor.

consists of 16 equally spaced electrodes, which are flush mounted at the periphery of each sensor plane.

The sensor planes are separated by an axial distance of 50 mm to realise the application of the cross-correlation dispersed-phase velocity profiling method. All the subsystems are integrated and positioned with consideration to their contribution into the final phase flow rate measurement. The effective measuring region of the ERT sensor is located between all the other sensors at the downstream of the whole multiphase measurement system. The differential pressure sensors are used to measure the pressure difference along the whole system. Two absolute pressure transducers are used to measure the absolute pressures at two locations (high pressure point and low pressure point) within the section, the values of which are also used for the correction of gas density. A blank flanged pipe section is mounted on the flowmeter section to increase the length of the system and realise a more accurate measurement of differential pressure along the section. A temperature transducer is positioned at the downstream end of the ERT to measure the temperature of the three-phase mixture.

2.2. Integration of DFM

This section highlights the detailed use of DFM and its integration in the three-phase flow metering technique. The measurement model is developed based on the initial assumption that the dispersed phase measured by the ERT consists of oil and gas phase. The ERT with dual plane sensors is used to extract the dispersed phase local volume fraction distribution and the dispersed phase local flow velocity. The online measurement of local velocity distribution is based on the pixel-pixel cross-correlation.

The gradiomonometer FDM is employed along with ERT to estimate the mixture density ρ_m^{FDM}, based on the Darcy–Weisbach equation [14], as shown in equation (10):

$$\rho_m^{\mathrm{FDM}} = \frac{\Delta P}{h_p\left[g\cos\theta + \frac{2C_f V_m^2}{D}\right]} \tag{10}$$

where C_f is the fanning friction factor, which is a function of Reynolds number (Re) and relative roughness; V_m is the mixture velocity assumed to be $V_{d-\mathrm{ERT}}$. h_p is the pipe height and D is the pipe diameter.

The mixture density ρ_m^{FDM} is calculated using the homogeneous model shown in equations (11)–(13), in which the subscript C denotes the continuous phase (water):

$$\rho_m^{FDM} = \bar{\alpha}_G\rho_G + \bar{\alpha}_O\rho_O + \bar{\alpha}_C\rho_C \tag{11}$$

$$\bar{\alpha}_d + \bar{\alpha}_C = 1 \tag{12}$$

Rearranging equation (11) to obtain equation (13):

$$\rho_m^{\mathrm{FDM}} = (\bar{\alpha}_d - \bar{\alpha}_O)\,\rho_G + \bar{\alpha}_O\rho_O + (1-\bar{\alpha}_d)\,\rho_C \tag{13}$$

Then the volume fraction of each phase can be determined, using equations (1)–(3).

In order to take the slip velocity into account, DFM is combined with the ERT and FDM system. In the integration of DFM a two-step approach is taken. The first step assumes the three-phase flow as two-phase flow, gas and liquid, where the oil–water mixture is handled as a pseudo-homogenous liquid. The second step extends the liquid phase to a two-phase mixture, oil and water. Equation (14) [15] expresses the DFM, describing the relative motion in the mixture between two phases (gas–liquid or liquid–liquid):

$$v_p = C_o V_m + V_p' d \tag{14}$$

where, V_m is the mixture velocity in m s^{-1}, $V_p' d$ is the phase drift velocity in m s^{-1} and C_o is a non-dimensional distribution parameter. The distribution parameter, C_o, is determined assuming that the flow is a fully developed bubbly flow and that C_o is dependent on the density ratio between the two phases (gas and liquid) and on the Reynolds number, Re. The

density group scales the inertia effects of each phase in a transverse void distribution. Considering a wide range of Reynolds number and a fully developed bubbly flow, in which the void fraction is beyond the range of $0 < \alpha < 0.25$ [16], the distribution parameter is estimated using equation (15):

$$C_o = \left(1.2 - 0.2\sqrt{\frac{\rho_g}{\rho_l}}\right) \tag{15}$$

The drift velocity $V_p'd$ is determined based on the size and physical property of the bubbles, large enough to rise in a stationary liquid [17]. The average mixture velocity, V_m, is the sum of the phase superficial velocities, for example in gas and liquid phase $V_m = V_{sg} + V_{sl} = \bar{\alpha}_g v_g + \bar{\alpha}_l v_l$, where the subscript s denotes superficial.

Equations (16) and (17) show the relative relationship between the gas and liquid phases:

$$v_g = v_r + v_c \tag{16}$$

$$V_m = \bar{\alpha}_d v_d + \bar{\alpha}_c v_c \tag{17}$$

Combining equations (16) and (17) we obtain equation (18):

$$V_m = (v_g - v_r)\,\bar{\alpha}_c + v_d \bar{\alpha}_d \tag{18}$$

where the relative velocity, v_r, which is a function of gas drift velocity, $V_g'd$, between gas–liquid is calculated using equation (19):

$$v_r = V_g'd/\,(1 - \alpha_g)\,. \tag{19}$$

The corresponding drift flux velocity for gas–liquid is calculated using equation (20):

$$V_g'd = 1.53 v_c'(1 - \bar{\alpha}_g)^2 \tag{20}$$

where v_c' is the characteristic velocity, which is described based on fluid property; and expressed using equation (21) [18]:

$$v_c' = \left[\frac{\sigma g\,(\rho_l - \rho_g)}{{\rho_l}^2}\right]^{1/4} \tag{21}$$

where, ρ_l, σ, g are liquid density, surface tension and gravitational acceleration, respectively. The liquid (oil and water) density, ρ_l, is determined using equation (22):

$$\rho_l = (\bar{\alpha}_{ol}\rho_o + \bar{\alpha}_{wl}\rho_w) \tag{22}$$

The oil and water volume fractions in the liquid phase, $\bar{\alpha}_{ol}$ and $\bar{\alpha}_{wl}$, are calculated using $\bar{\alpha}_{pl} = \frac{\bar{\alpha}_p}{\bar{\alpha}_w + \bar{\alpha}_o}$ [15]. Where $\bar{\alpha}_o$ and $\bar{\alpha}_w$ are the mean oil and water volume fractions, repectively, and determined by equations (2) and (3) from combination of the FDM and the ERT data.

Similarly, using the basic expression of the two-phase DFM to deduce the velocity of water and oil within the oil–water system. Equations (23) and (24) show the mixture velocity, V_m, and liquid mixture velocity, V_{sl}, respectively:

$$V_m = V_{sl} + \bar{\alpha}_g v_g \tag{23}$$

$$V_{sl} = \bar{\alpha}_{ol} v_o + \bar{\alpha}_{wl} v_w \tag{24}$$

Substituting V_m, in the gas drift flux expression to obtain equation (25):

$$V_{sl} = \frac{v_g\,(1 - C_o\bar{\alpha}_g) + V_g'd}{C_o} \tag{25}$$

Equations (26) and (27) show the relative relation between oil and water phase:

$$v_o = v_r' + v_w \tag{26}$$

$$\frac{V_{sl} - \bar{\alpha}_{wl} v_w}{\bar{\alpha}_{ol}} = v_r + v_w \tag{27}$$

where the oil–water relative velocity, v_r', is determined using $v_r' = V_o'd/\,(1 - \bar{\alpha}_{ol})$. Thus, the oil drift velocity, $V_o'd$, is calculated using equation (28):

$$V_o'd = 1.53 v_c'(1 - \bar{\alpha}_{ol})^2 \tag{28}$$

where the characteristic velocity v_c' for oil–water system is expressed by equation (29):

$$v_c' = \left[\frac{\sigma_{ow} g\,(\rho_w - \rho_o)}{\rho_w^2}\right]^{1/4} \tag{29}$$

where, σ_{ow} is the oil–water surface tension taken as 0.0335 N m^{-1}.

Substituting the above quantities in equations (4)–(6), yields the velocities of oil, gas and water.

3. Performance of ERT-FDM-DFM method

The flow measurement results obtained from the proposed method are analysed and compared to the reference values used in the previously published paper by Wang *et al* [7] The measured phase volume flow rates are determined using equations (7)–(9), based on phase volume fractions and the velocities calculated by equations (1)–(6).

Figure 3 shows the comparison of the measured oil volume flow rate with that of the reference. It can be seen that the measured values are in a good agreement with the reference values. By observing the measured oil flow rate values, it is clear that a larger deviation from the measured values can be seen with the increase of the oil flow rates. This is due to the fact that, by increasing the oil flow rate, the flow becomes oil continuous, and a layer of nonconductive oil covers the electrodes mounted on each ERT plane.

According to figure 4, it is apparent that the measured water flow rate values agree well with the references values. However, deviations from the reference values can be seen as the volumetric flow rate increases. This may be attributed to errors

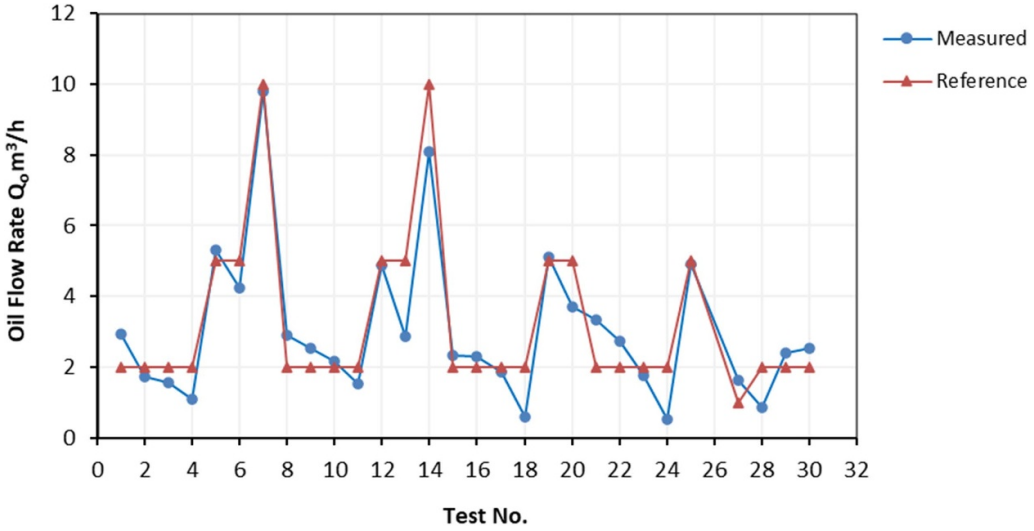

Figure 3. Measured oil flow rate vs reference oil flow rate.

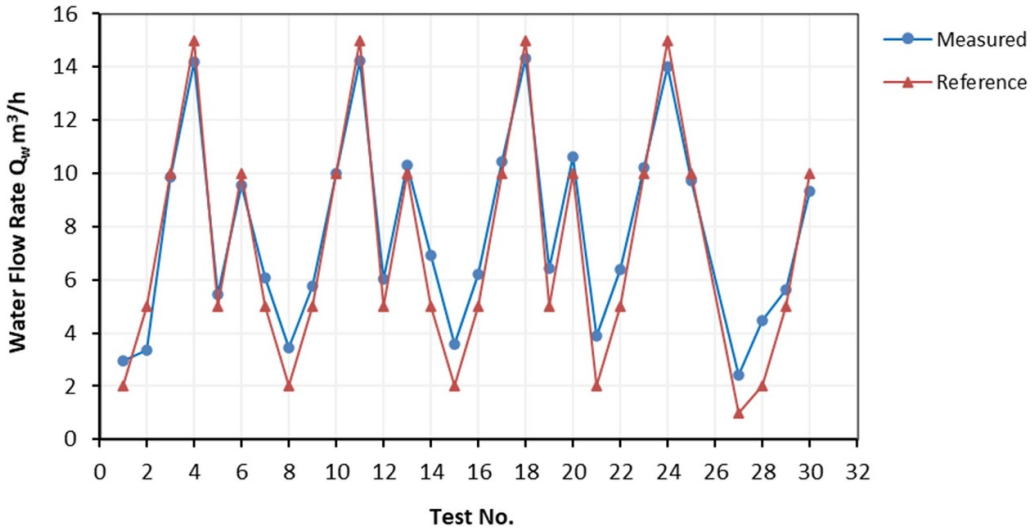

Figure 4. Measured water flow rate vs reference water flow rate.

in mean volume fraction and/or velocity values. The verification of this cause and the errors associated with volume fraction and/or velocity is the subject of future investigation.

Figure 5 compares the measured gas volume flow rate with that of the reference values. The measured values follow similar trend as those of the reference, with a clear deviation from the reference values. By observing the trend, it is apparent that the level of deviation pronounced at high gas flow rates is higher than that at low levels. This is expected due to the limitation of the ERT in handling higher gas flow rates, at which the electrodes may not all be in contact with the continuous conductive water phase.

The ERT is known to be flow regime dependent and suffer from a weak resolution in the centre region of the pipe flow. However, it is important to point out that only the small area in the centre of the pipe (ca. 3%–5% of the pipe cross-section) may be affected by this limitation. In this study the measurement results of bubbly flow (tests 1–11) seem to be less affected as opposed to slug flow, in which Taylor bubbles exist and occupy approximately the entire pipe cross-section.

The weak resolution of the ERT and the issues of distinguishability (particularly at the boundary region) may limit its use for visualisation of prevailing flow regime. This can be seen in figure 6(a) bubbly flow and 6(b) slug flow reconstructed tomograms with the modified sensitivity back projection algorithm (MSBP). It is worth pointing out that these tomograms represent typical special features of the flow. The conductivity data correspond to the above two tomograms are part of the results of a project (ENG58-EMRP), which used the same test results obtained from SGR flow facility. It can be seen that the colour mapping of the reconstructed tomograms

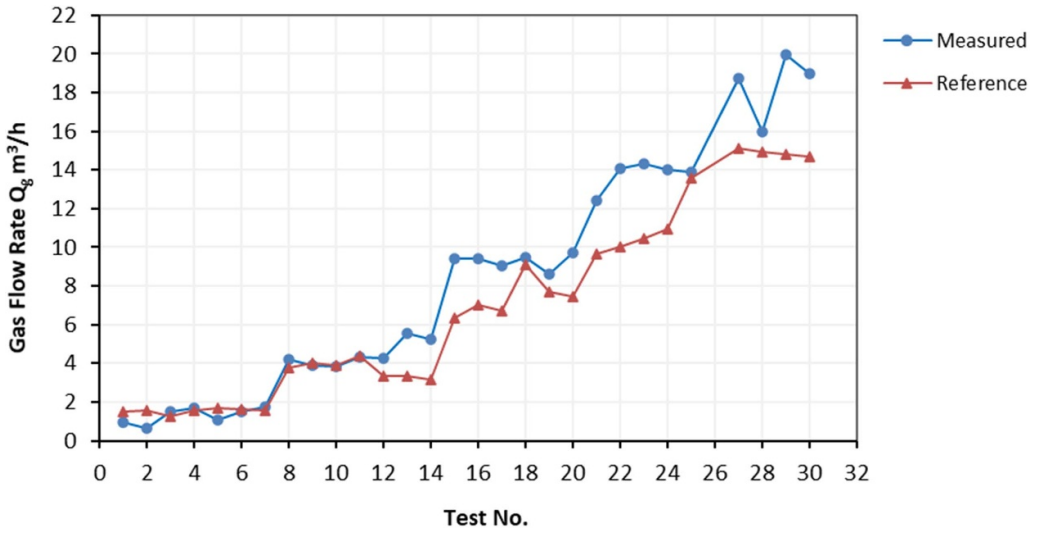

Figure 5. Measured gas flow rates vs reference gas flow rate.

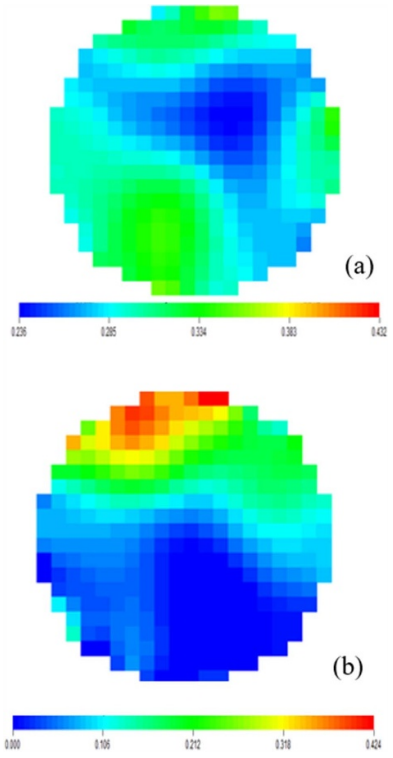

Figure 6. ERT conductivity tomograms of bubble flow (a) and slug flow (b) reconstructed using MSBP.

from the ERT are not able to demonstrate sufficient flow characteristics. This is due to the incapability of the ERT to reveal the conductivity change within certain region.

It is known that the bubble size affects the void fraction as well as the distribution parameter, then it may be reasonable to expect that the slip velocity of rising bubbles to be dependent on the bubble size. Bubbly flow is described as small bubbles (typically 1–6 mm) dispersed in the liquid phase and slug flow is characterised by the presence of large Taylor bubbles with sizes in the order of the pipe diameter. Based on the above discussion, the higher deviation of measured gas flow rates from reference values could also be due to the fact that at higher gas flow rates, where slug flow occurs, the slip velocity is not taken into account, as a result the gas flow rate measurements are affected. Perhaps this is attributed to the errors associated with the distribution parameter, which is calculated using a bubbly flow equation, equation (15), and may not be applicable to slug flow. To address this issue, perhaps an approach that takes bubble size into account is needed for calculation of distribution parameter. On the other hand, the slip velocity between oil and water, where oil droplets are dispersed in the water phase, is typically very small. This implies that the oil and water travel at approximately the same velocity, as a result a negligible effect of slip velocity can be noticed in both oil and water flow rate measurements.

Further evaluation of ERT-FDM-DFM measurement strategy is carried out, in which the measured water liquid ratio (WLR) is compared with that of the reference, as shown in figure 7. The WLR is determined based on the volume flow rate of oil and water, Q_o and Q_w, respectively. Figure 7 shows a comparison of results between the measured and reference WLR values as a function of GVF. It can be seen in figure 7 that the measured values are associated with $\pm 10\%$ absolute error, demonstrating that the ERT-FDM-DFM flow measurement strategy provides a reasonably accurate and reliable results.

To further illustrate the uncertainties associated with the measured results, the WLR vs GVF composition map is constructed, as shown in figure 8. It is worth mentioning that the evaluation of the measurement results carried out is based on the range of conditions used in this study. The effects of conditions that do not fall within the range of temperature and pressure mentioned in the test condition table is beyond the scope of this study.

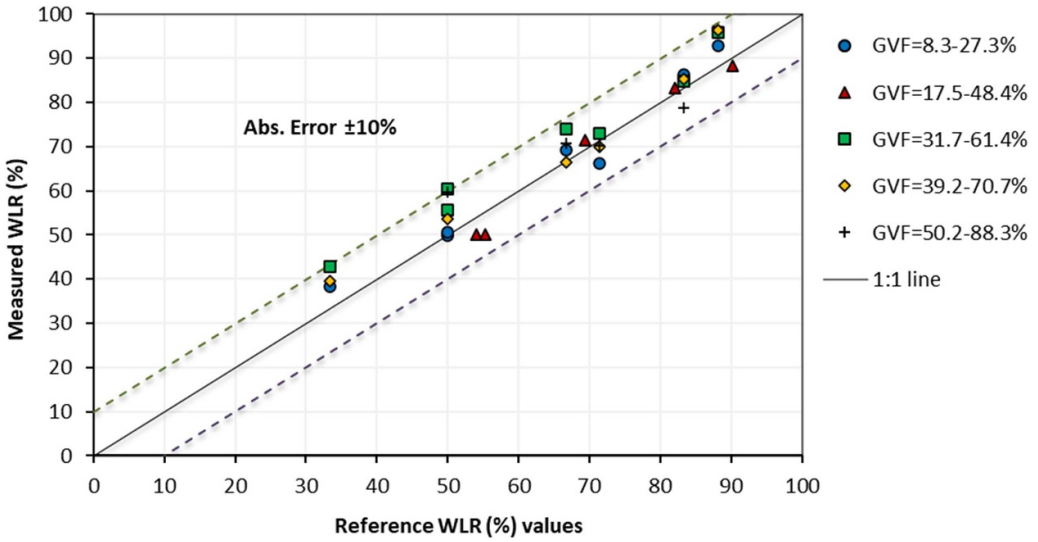

Figure 7. Measured WLR vs reference WLR.

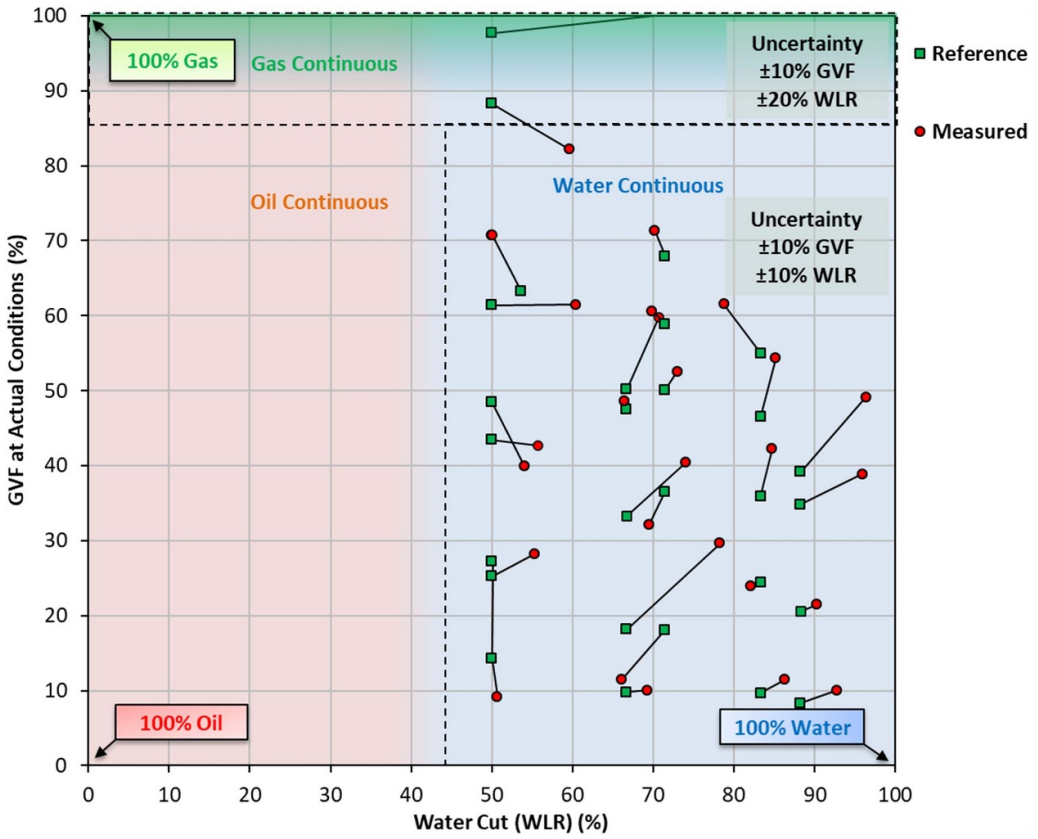

Figure 8. Composition map of oil–gas–water flow.

The oil, gas and water continuous regions are illustrated as red, green, and blue shades, respectively. The reference values are indicated by green data series, whereas the measured values are indicated by red data series. The reference values are connected to the corresponding measured values in the composition map, indicating the error percentage from the projected length. By observing the map, it can be seen that ±10% uncertainty in WLR and GVF lies within the range of 45%–100% WLR and 9%–85% GVF. It is clear that as the GVF increases above 85%, which is within the gas-continuous region, the performance of the measurement strategy deteriorates and the WLR measurement uncertainty reaches ±20%. This is attributed to the limitation of ERT in handling high GVF.

4. Conclusions

This paper demonstrates the performance of a novel method, using ERT-FDM-DFM measurement system, for measuring phase volume flow rate of oil–gas–water upward vertical flow within water-continuous region. Based on the results, a reasonable agreement between the measured and the reference values can be noted. However, a significant deviation presents in some cases, particularly at high gas flow rates.

The results indicate that the developed ERT-FDM-DFM measurement provides good performance at WLR > 45% and GVF range of 9%–85%, with an absolute error of ±10%. It can be concluded that the strategy achieves a reasonably accurate, reliable and consistent measurement of phase flow rates. The proposed ERT-FDM-DFM offers a non-invasive and rapid measurement, in which phase flow rates are determined, considering slip velocities. Moreover, the proposed measurement system, in which the DFM is integrated can operate without using multiple expensive instruments thereby reducing both capital and maintenance costs. It is expected that the proposed multi-modality ERT-FDM-DFM has the potential to be implemented in transportation pipelines, oil production lines and many other business critical processing equipment items.

Data availability statement

No new data were created or analysed in this study.

Acknowledgments

This work was supported by the European Metrology Research Programme (EMRP). The authors would like to thank Dr Qian Wang, from the University of Edinburgh for the contribution of providing the data from ENG58-EMRP Report.

ORCID iDs

Sara Rashed https://orcid.org/0000-0003-1518-0596
Yousef Faraj https://orcid.org/0000-0003-4418-3649

References

[1] Faraj Y, Wang M, Jia J, Wang Q, Xie C, Oddie G, Primrose K and Qiu C 2015 Measurement of vertical oil-in-water two-phase flow using dual-modality ERT–EMF system *Flow Meas. Instrum.* **46** 255–61
[2] Kjølaas J, Belt R, Wolden M, Schümann H and Richon V 2021 Experiments and modelling of three-phase vertical pipe flow *Chem. Eng. Sci.* **247** 117091
[3] Shi X, Tan C, Dong F and Escudero J 2021 Flow rate measurement of oil-gas-water wavy flow through a combined electrical and ultrasonic sensor *Chem. Eng. J.* **427** 131982
[4] Ma Y, Li C, Pan Y, Hao Y, Huang S, Cui Y and Han W 2021 A flow rate measurement method for horizontal oil-gas-water three-phase flows based on Venturi meter, blind tee, and gamma-ray attenuation *Flow Meas. Instrum.* **80** 101965
[5] Roshani M, Sattari M, Muhammad Ali P, Roshani G, Nazemi B, Corniani E and Nazemi E 2020 Application of GMDH neural network technique to improve measuring precision of a simplified photon attenuation based two-phase flowmeter *Flow Meas. Instrum.* **75** 101804
[6] Hansen L, Pedersen S and Durdevic P 2019 Multi-phase flow metering in offshore oil and gas transportation pipelines: trends and perspectives *Sensors* **19** 2184
[7] Wang M, Jia J, Faraj Y, Wang Q, Xie C, Oddie G, Primrose K and Qiu C 2015 A new visualisation and measurement technology for water continuous multiphase flows *Flow Meas. Instrum.* **46** 204–12
[8] Qureshi M, Ali M, Ferroudji H, Rasul G, Khan M, Rahman M, Hasan R and Hassan I 2021 Measuring solid cuttings transport in Newtonian fluid across horizontal annulus using electrical resistance tomography (ERT) *Flow Meas. Instrum.* **77** 101841
[9] Razzak S, Barghi S and Zhu J 2007 Electrical resistance tomography for flow characterisation of a gas–liquid–solid three-phase circulating fluidised bed *Chem. Eng. Sci.* **62** 7253–63
[10] Ishii M and Hibiki T 2006 *Thermo-fluid Dynamics of Two-Phase Flow* (Berlin: Springer)
[11] Abam F, Dilibe N, Nwankwojike B, Diemuodeke O and John I 2021 Comparative evaluation of homogenous and drift-flux models for a three-phase downward flow in a pipe *Sci. Afr.* **13** e00898
[12] Soprana B, Ribeiro G, Saliva A and Maliska C 2012 Numerical solution of the multiphase flow of oil water and gas in horizontal wells in natural petroleum reservoir *Mecánica Computacional* (*Salta, Argentina*, *13–16 November 2012*) pp 683–93
[13] Dong C, Rassame S, Zhang L and Hibiki T 2020 Drift-flux correlation for upward two-phase flow in inclined pipes *Chem. Eng. Sci.* **213** 115395
[14] Chanson H 2004 *The Hydraulics of Open Channel Flow* (Amsterdam: Elsevier Butterworth-Heinemann)
[15] Shi H, Holmes J, Diaz L, Durlofsky L and Aziz K 2005 Drift-flux parameters for three-phase steady-state flow in wellbores *SPE J.* **10** 130–7
[16] Hibiki T and Ishii M 2002 Distribution parameter and drift velocity of drift-flux model in bubbly flow *Int. J. Heat Mass Transfer* **45** 707–21
[17] Falcone G, Hewitt G and Alimonti C 2009 *Multiphase Flow Metering* vol 1–15 (Amsterdam: Elsevier) pp 30–40
[18] Azbel D 2009 *Two-Phase Flows in Chemical Engineering* (Cambridge: Cambridge University Press)